$T.\ Hirota,\ H.\ Imai,\ K.\ Menten,\ &\it Y.\ Pihlstr\"{o}m,\ eds.$

doi:10.1017/S1743921323002272



Kinematics in the Galactic Center with SiO masers

Jennie Paine and Jeremy Darling

Center for Astrophysics and Space Astronomy, Department of Astrophysical and Planetary Sciences University of Colorado, 389 UCB, Boulder, CO 80309-0389, USA.

email: jennie.paine@colorado.edu

Abstract. Stellar SiO masers are found in the atmospheres of asymptotic giant branch (AGB) stars with several maser transitions observed around 43 and 86 GHz. At least 28 SiO maser stars have been detected within ~2 pc projected distance from Sgr A* by the Very Large Array (VLA) and Atacama Millimeter/submillimeter Array (ALMA). A subset of these masers have been studied for several decades and form the basis of the radio reference frame that anchors the reference frame for infrared stars in the Galactic Center (GC). We present new observations of the GC masers from VLA and ALMA. These new data combined with extant maser astrometry provide 3D positions, velocities, and acceleration limits. The proper motions and Doppler velocities are measured with unprecedented precision for these masers. We further demonstrate how these measurements may be used to trace the stellar and dark matter mass distributions within a few pc of Sgr A*.

Keywords. Silicon monoxide masers, stellar masers, Galactic Center, stellar kinematics

1. Introduction

Stellar kinematics probe the gravity profile in which the stars reside, which in the centers of galaxies will be dominated by a supermassive black hole, stars, and dark matter. The dark matter profiles in galactic centers are particularly of interest due to the discrepancy between simulations, which predict steep profiles (cusps), and observations, which find flat profiles (cores). This difference is known as the core-cusp problem (see de Blok 2010 for a review). Dark matter profiles on scales of several parsec and smaller are additionally poorly constrained by both simulations and observations.

The question of the distribution of dark matter in galactic centers is also tied to the presence and growth of the central black hole. If the supermassive black hole grows adiabatically, then the dark matter profile will steepen within the sphere of influence of the black hole (Gondolo & Silk 1999), known as a dark matter spike, and stars respond similarly to the presence of a black hole. The stellar cusp in our galaxy is shallower than predicted by theory (Schödel et al. 2018; Habibi et al. 2019), suggesting the absence of a dark matter spike, but the two profiles are not necessarily coupled if the stellar cluster formed after the growth of the black hole.

Determining the distribution and kinematics of stars in the Galactic Center (GC) is challenging due to high extinction and stellar crowding, but radio observations are unaffected by these issues. Thus, one can use stellar maser emission detected at radio frequencies to uniquely measure stellar kinematics with high resolution within a several parsec range around the central galactic black hole Sgr A*. We present observations of the 43 and 86 GHz masers in the GC from the Very Large Array (VLA) and the Atacama Large Millimeter/submillimeter Array (ALMA), and their resulting kinematics over several decades of observations. We show that the velocities and accelerations of

[©] The Author(s), 2024. Published by Cambridge University Press on behalf of International Astronomical Union. This is an Open Access article, distributed under the terms of the Creative Commons Attribution licence (http://creativecommons.org/licenses/by/4.0/), which permits unrestricted re-use, distribution and reproduction, provided the original article is properly cited.

these stars may be used to constrain the mass distribution around Sgr A*, though the measurements are complicated by the intrinsic variability of stellar SiO masers. Finally, we discuss the results of recent GC maser observations.

2. Stellar SiO masers in the Galactic Center

Sgr A* is the supermassive black hole at the center of our galaxy and a bright, compact radio source. The first strong evidence for the existence of the black hole was provided by near-infrared (near-IR) observations of stars on short period orbits around Sgr A* (Ghez et al. 2000, 2005; Schödel et al. 2002; Eisenhauer et al. 2005). The orbits of these "S" stars suggest a black hole mass of $4.15 \times 10^6~M_{\odot}$ and a distance to the GC of 8.2 kpc Ghez et al. (2008); Genzel et al. (2010). Additionally, following the pericenter passage of S2 — a star on a highly eccentric orbit with pericenter at 120 AU from Sgr A* (approximately 1400 times the black hole's event horizon) — IR stellar orbits were able to test General Relativity (e.g. gravitational redshift and Schwarzschild precession; GRAVITY Collaboration et al. 2018; Do et al. 2019; GRAVITY Collaboration et al. 2020).

Since there is no obvious, bright near-IR counterpart source to Sgr A* from which to reference the positions of S stars, the IR stellar orbit measurements rely on the definition of an astrometric reference frame. Recently, the reference frame has been defined using the proper motions of SiO maser-emitting stars in the vicinity of Sgr A*, since the masers are observed in radio frequencies where the Sgr A* radio source is also detected. Observations of the GC over the past several decades have identified at least 28 stellar SiO masers within a few parsecs of Sgr A* (e.g. Menten et al. 1997; Reid et al. 2007; Li et al. 2010; Borkar et al. 2020; Paine & Darling 2022), and a subset of these maseremitting stars are bright IR sources used for the reference frame. Menten et al. (1997) first proposed measuring the SiO proper motions relative to the Sgr A* radio continuum and matching the radio positions to the IR counterparts to determine the location of Sgr A* in IR images and establish a reference frame where Sgr A* is at rest. Since then, several iterations of the reference frame have been determined using SiO maser proper motions (e.g. Menten et al. 1997; Reid et al. 2007; Yelda et al. 2010; Sakai et al. 2019). The advantage of the radio reference frame is that as proper motion uncertainties decrease in time by $t^{-3/2}$, so does the reference frame improve. However, projecting the maser proper motions forward in time is a large source of uncertainty in the reference frame and resulting IR orbital measurement, so continuous monitoring of the SiO masers is required to improve the precision of IR measurements.

Stellar masers typically occur in the extended atmospheres and circumstellar envelopes of red giants and asymptotic giant branch (AGB) stars. SiO emission is found closest to the star compared to other maser lines, at radii of \sim a few AU, interior to the dust formation point which drives the stellar wind. The observed SiO maser lines are rotational transitions typically in excited vibrational states. Several SiO lines are observed at frequencies around 43 GHz (J=1-0) and 86 GHz (J=2-1). VLBI observations of stellar SiO masers typically resolve the emission into discrete spots in a ring-like structure around the star which may be variable over relatively short timescales (e.g. Gonidakis et al. 2013). Individual maser spots track the local motion of material around the star, which is not always symmetric, and components may turn on or off between observations. The variability of the maser components may be caused by changes in the dominant pumping mechanism or acceleration of the maser medium with respect to the star disrupting the requirement of velocity coherence.

The result for lower resolution observations which detect the aggregate maser emission of many components is that SiO maser spectra often show multiple peaks distributed over a velocity range of $\sim 10 \text{ km s}^{-1}$ relative to the systemic stellar velocity (Jewell *et al.* 1991),

and which may vary in time. Different maser transitions observed simultaneously may not match in the location of spectral peaks since the transitions are not necessarily coincident around the star. Maser variability will also introduce intrinsic scatter in the astrometry over time as the position centroid may move around the area of maser ring.

3. Current maser kinematic measurements

In Paine & Darling (2022), we presented five epochs of observations of stellar SiO masers in the GC using VLA and ALMA. Interferometers like VLA and ALMA do not measure images of the sky directly, but instead sample the Fourier transform of the sky brightness, known as the visibilities. In cases where the observed source can be represented with a simple model (or a linear combination of simple models as in the case of a sample of point sources), one may forgo the creation of images and instead fit to the visibilities (e.g. Martí-Vidal et al. 2014; see also Pearson 1995 for a discussion of visibility model fitting and its applications). We use visibility fitting of the masers' positions and spectra to maximize the resolution of the observations — the smallest resolvable angular size is smaller than the diffraction limit of the interferometer for high signal-to-noise sources — and to minimize systematic differences from comparing data between different epochs and telescopes.

Combined with extant maser astrometry, we found proper motions and proper accelerations for the GC maser sample. The corresponding 2D stellar maser kinematics are measured with $0.5~\rm km~s^{-1}$ and $0.04~\rm km~s^{-1}~yr^{-1}$ precision for velocities and accelerations, respectively. The radial velocities and accelerations are measured with $0.5~\rm km~s^{-1}$ and $0.1~\rm km~s^{-1}~yr^{-1}$ precision, respectively. These measurements are the current benchmark for the published kinematics of these stars, though the precision and accuracy of the kinematics are heavily impacted by the intrinsic variability of the SiO maser sources, as described above.

By modeling the expected kinematics of stars in circular orbits about the GC, we identified several stars with anomalous velocity or acceleration measurements which are significantly higher than anticipated (discussed below). Figure 1 shows the 3D acceleration measurements and velocity-based enclosed mass limits for our sample of stars as a function of projected distance from Sgr A*. We compare these to models of the total mass profile, both with and without a theoretical dark matter spike, to demonstrate how the maser kinematics may differentiate between dark matter models in the GC with improved precision from more observations.

4. Implications from continued maser monitoring

Since the publication of Paine & Darling (2022), we have observed one additional epoch from VLA and one from ALMA, which generally improve the precision of the kinematic measurements. Several anomalous velocities or accelerations are also confirmed using the new observations. For example, the stars SiO-16, SiO-21, and SiO-25 (the outlying stars in the upper right of the left figure of Figure 1) have proper motion-based velocities > 1000 km s⁻¹, which are about an order of magnitude larger than anticipated for their locations in the GC. These large velocities may be the product of measurement error or incorrect distance estimates if the stars are actually located in the foreground rather than the GC. However, if accurate, these velocities would suggest that the stars are not bound to the GC.

Additionally, several stars, such as SiO-14 and IRS 15NE, show significant or marginally significant acceleration in the velocity centroid of the maser spectra over time which cannot be explained by acceleration of the star about the GC alone. As noted in Section 2, SiO maser spectra are highly variable about the systemic stellar velocity and

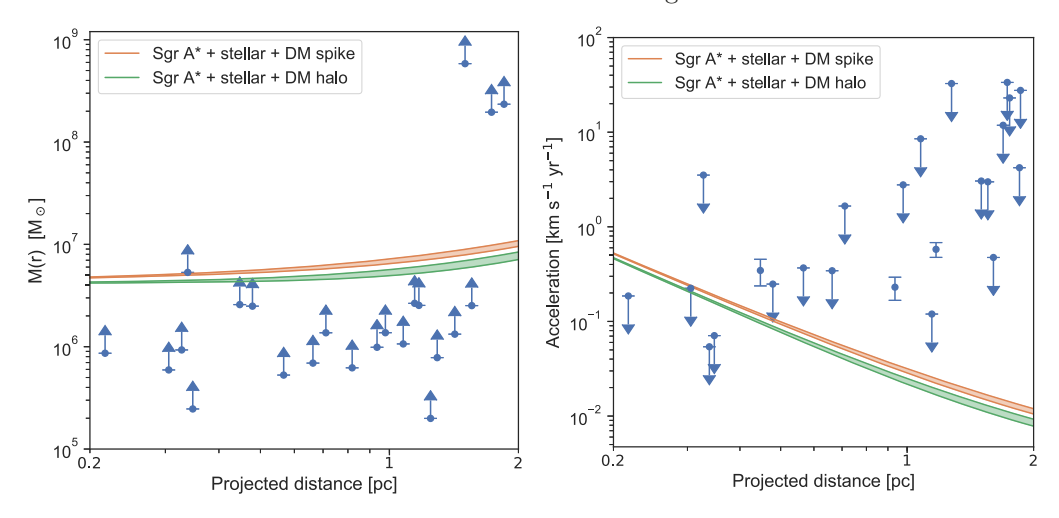


Figure 1. Figures adapted from Paine & Darling (2022). Left: Enclosed mass lower limits calculated from the stellar 3D velocities as a function of projected distance. The dark matter halo model (green region) is a generalized NFW profile (McMillan 2017), and the maximal dark matter spike model (orange region) includes an additional sharp spike in the dark matter density profile (Lacroix 2018). Right: 3D stellar acceleration magnitude upper limits as a function of projected distance. Shaded regions show expected accelerations due to models of the interior stellar and dark matter mass. Error bars indicate stars with at least 3σ measurement of the total acceleration.

therefore acceleration of the aggregate maser source may not reflect real acceleration of the star. However, one would expect to observe this as scatter about the trend, so the large, approximately secular changes in velocity observed for these stars requires further investigation.

References

Borkar, A., Eckart, A., Straubmeier, C., et al. 2020, Multifrequency Behaviour of High Energy Cosmic Sources - XIII, 33

de Blok, W. J. G. 2010, Advances in Astronomy, 2010, 789293

Do, T., Hees, A., Ghez, A., et al. 2019, Science, 365, 664

Eisenhauer, F., Genzel, R., Alexander, T., et al. 2005, ApJ, 628, 246

Genzel, R., Eisenhauer, F., & Gillessen, S. 2010, Reviews of Modern Physics, 82, 3121

Ghez, A. M., Morris, M., Becklin, E. E., et al. 2000, Nature, 407, 349

Ghez, A. M., Salim, S., Hornstein, S. D., et al. 2005, ApJ, 620, 744

Ghez, A. M., Salim, S., Weinberg, N. N., et al. 2008, ApJ, 689, 1044

Gondolo, P. & Silk, J. 1999, Phys. Rev. Lett., 83, 1719

Gonidakis, I., Diamond, P. J., & Kemball, A. J. 2013, MNRAS, 433, 3133

GRAVITY Collaboration, Abuter, R., Amorim, A., et al. 2018, A&A, 615, L15

GRAVITY Collaboration, Abuter, R., Amorim, A., et al. 2020, A&A, 636, L5

Habibi, M., Gillessen, S., Pfuhl, O., et al. 2019, ApJ (Letters), 872, L15

Jewell, P. R., Snyder, L. E., Walmsley, C. M., et al. 1991, A&A, 242, 211

Lacroix, T. 2018, A&A, 619, A46

Li, J., An, T., Shen, Z.-Q., et al. 2010, ApJ (Letters), 720, L56

Martí-Vidal, I., Vlemmings, W. H. T., Muller, S., et al. 2014, A&A, 563, A136

McMillan, P. J. 2017, MNRAS, 465, 76

Menten, K. M., Reid, M. J., Eckart, A., et al. 1997, ApJ (Letters), 475, L111

Paine, J. & Darling, J. 2022, ApJ, 927, 181

Pearson, T. J. 1995, Very Long Baseline Interferometry and the VLBA NRAO Workshop No. 22, Astronomical Society of the Pacific Conference Series, 82, 267

Reid, M. J., Menten, K. M., Trippe, S., et al. 2007, ApJ, 659, 378 Sakai, S., Lu, J. R., Ghez, A., et al. 2019, ApJ, 873, 65 Schödel, R., Ott, T., Genzel, R., et al. 2002, Nature, 419, 694 Schödel, R., Gallego-Cano, E., Dong, H., et al. 2018, $A\mathcal{E}A$, 609, A27 Yelda, S., Lu, J. R., Ghez, A. M., et al. 2010, ApJ, 725, 331